

УДК 539.17.1

PROPERTIES OF THE HADRONIC JETS IN $\pi^- + p$ AND $\pi^- + C$ INTERACTIONS AT 40 GeV/c

A. A. Kuznetsov^a, Yu. A. Panebrattsev^a, R. Togoo^b, B. Baatar^a

^a Joint Institute for Nuclear Research, Dubna

^b Institute of Physics and Technology, Ulaanbaatar, Mongolia

The charged π -meson and proton mixed hadronic jets in the fragmentation regions of $\pi^- + p$ and $\pi^- + C$ interactions at 40 GeV/c are extracted and their properties are investigated. It has been shown that the characteristics of the jets in π^- -meson fragmentation region are universal in jet events, do not depend on the type of the target and are defined only from the quark contents of the π^- meson. The jet characteristics in the proton fragmentation region are different and depend upon the quark contents of the proton. Mixed hadronic jets with defined value of the electric charge were studied. The resonance structures related with the Δ isobars are discovered in the effective mass distributions of the jets. It has been shown that the small azimuthal angle high- p_T correlations are observed and strong back-to-back correlations exist.

Выделены «смешанные» адронные струи, т. е. струи, состоящие из заряженных π^\pm -мезонов и протонов, в π^-p - и π^-C -взаимодействиях при импульсе π^- -мезона 40 ГэВ/с в областях фрагментации взаимодействующих частиц и исследованы их свойства. Показано, что характеристики струй в области фрагментации начального π^- -мезона универсальны в одноструйных и двухструйных событиях, они не зависят от вида мишени и определяются кварковым составом π^- -мезона, а характеристики струй в области фрагментации протона существенно другие и определяются кварковым составом протона. Изучены смешанные адронные струи с определенным значением электрического заряда. Обнаружено, что в распределениях по эффективной массе таких струй наблюдаются резонансные структуры, связанные с Δ -резонансами. Показано, что наблюдаются малые азимутальные корреляции с большими p_T и существуют сильные корреляции вперед-назад.

INTRODUCTION

Interest in studying soft hadron-hadron processes characterized by small transverse momenta of produced particles is connected with an attempt to describe these processes based on the quark-parton structure of hadrons. To describe such processes, a number of recombination-type models have been developed in which the quark-parton distribution functions of an incoming hadron are related to the production inclusive cross sections of fast or leading particles in the fragmentation regions of interacting hadrons [1–3].

An experimental observation of approximate similarity of the distribution function of proton valence quarks determined from deep-inelastic leptonic process and the inclusive spectra of proton fragmentation into π^\pm mesons has served as a main motivation of such an approach [4, 5]. In the framework of these models, the pions are produced due to the recombination of a last valence quark and a low-energy antiquark from the composition of an initial proton.

Similarity of the spectra of leading hadrons and the distribution functions of valence quark (or antiquarks) in interacting hadrons is also reproduced in the framework of coalescence model of interacting hadrons. However, it should be remembered that the kinematics of hadron production is significantly different within the framework of the recombination and coalescence models [6], and another scheme of quark hadronization is proposed in the framework of the fragmentation models.

If we turn from consideration of a leading hadron to a group of hadron, then it is expected that a leading hadron and some other hadrons nearest to it in rapidity may produce a group of hadrons (or a jet) which will have the same leading properties as well. For this reason, the characteristics of such a group of hadrons as a whole are determined by the quark distribution function and the quantum numbers of a quark fragmenting into this group of particles (or a jet). Proceeding from this, spectator hadron jet in soft processes can be defined as spatially isolated cluster of hadrons having leading properties; i.e., the group of hadrons carries information concerning a quark from the fragmenting hadron composition.

As distinct from leading hadrons, such characteristics as jet mass and charge and also particle multiplicity in a jet are not fixed values for hadron jets. It is naturally to expect that apart from the inclusive spectra of hadron jets, the properties of jet leadership should also appear in the distributions over these values.

To select hadron jets in multiparticle final state, the B algorithm used to study and reconstruct hadron jets is proposed in [7]. Positive invariant dimensionless quantities

$$b_{ik} = -(P_i/m_i - P_k/m_k)^2 \quad (1)$$

in relative 4-velocity space are used in this algorithm as a measure of closeness between particles i and k [8]. In this space, the hadron jet is defined as a group of points $u_i = P_i/m_i$ (each point corresponds to a real particle), and the distance between them (i.e., b_{ik}) is much smaller than the average distance between all the points of the set or the average distance between particles over the whole phase volume of the reaction. Besides B algorithm, A_n algorithm [9] and B_k algorithm [10] and minimum branching tree [11] are constructed in the basis of the b_k .

The logic of the B algorithm is constructed by complete analogy to that of the JADE algorithm [12–14]. The question on what differences these two algorithms can lead to is considered in [7] and in this paper below.

Based on the analysis of experimental data on multiple particle production in $\pi^- + p$ and $\pi^- + C$ interactions at 40 GeV/c, it is shown that hadron jets extracted by the B algorithm have the properties of leadership, and therefore they carry information on the characteristics of a quark owing to whose fragmentation they were produced.

1. RECONSTRUCTION OF MIXED HADRON JETS ON THE BASIS OF BINARY B ALGORITHM

This section is devoted to a study of the properties of a new binary B algorithm (see also [7]) used to search for and reconstruct hadron jets in multiple particle final states. The structure of logic organization of the B algorithm is the following:

a) For each event with N particles in the final hadron state (further, both one particle and a group of particles will be named a *precluster*), $N(N - 1)/2$ pair or binary characteristics

b_{ik} are defined [8]. They are distances in 4-velocity space between preclusters i and k with masses m_i and m_k and 4-momenta P_i and P_k , respectively. Here we naturally assume that $N \geq 2$.

b) A minimum value of $b_{i_{\min}k_{\min}} = \min \{b_{ik}\}$ is determined from $N(N-1)/2$ of quantities b_{ik} , i.e., a pair of preclusters i_{\min} and k_{\min} with a minimum distance in 4-velocity space is determined.

c) The obtained minimum value of $b_{i_{\min}k_{\min}}$ is compared to a predetermined quantity b_{cut} , which is a cut parameter of the B algorithm.

d) If $b_{i_{\min}k_{\min}} > b_{\text{cut}}$, the procedure of hadron jet reconstruction is completed.

e) If $b_{i_{\min}k_{\min}} < b_{\text{cut}}$, two preclusters i_{\min} and k_{\min} are joined in one precluster with mass $m_{i_{\min}k_{\min}}$ and 4-momentum

$$P_{i_{\min}k_{\min}} = P_{i_{\min}} + P_{k_{\min}} \quad (m_{i_{\min}k_{\min}}^2 = P_{i_{\min}k_{\min}}^2);$$

that is, the number of preclusters decreases by unity: $N \rightarrow (N - 1)$.

f) At $(N - 1) \geq 2$, the procedure is iterated for $(N - 1)$ preclusters. If $(N - 1) = 1$, the procedure of hadron jet reconstruction is completed.

g) All preclusters in which the number of particles is larger than or equal to 2 are considered as a hadron jet in given event.

From the foregoing it follows that the binary algorithm used to reconstruct hadron jets has three main elements:

- (i) a logic of the algorithm,
- (ii) a metric of the algorithm, and
- (iii) a cut parameter of the algorithm.

In particular, the B algorithm is based on particle collection in preclusters comparing a minimum distance between pairs of preclusters with algorithm cut parameter during each iteration (see the above mentioned items from (a) to (g)). The B algorithm metric is defined by expression (1), that is the distance between two preclusters i and k in 4-velocity space suggested in [8], and quantity b_{cut} is a cut parameter.

As was already noted, the B algorithm logic is constructed by complete analogy to the JADE collaboration algorithm used in search for hadron jets in e^+e^- interactions [12–14]. The difference between them lies in that the effective mass square of a pair of preclusters $m_{ik}^2 = (P_i + P_k)^2$ is used in the JADE algorithm instead of b_{ik} defining nearness between preclusters i and k and, accordingly, quantity m_{ik}^2 is a cut parameter m_{cut}^2 , i.e., the quantity with mass square dimensionality (or the same dimensionless quantity $y_{\text{cut}} = m_{\text{cut}}^2/s$, where \sqrt{S} is the energy in the center-of-mass system of collision). Note that quantities b_{ik} and m_{ik}^2 are bound by a simple relation, namely

$$b_{ik} = \frac{M_{ik}^2 - (m_i + m_k)^2}{m_i m_k}. \quad (2)$$

The algorithms constructed on their basis, i.e., the B and JADE algorithms, respectively, are completely different as shown in the sections below. Such a difference is due to the fact that the preclusters i and k of the quantities m_i and m_k , which enter into expression (2),

vary within the algorithm (i.e., from one iteration to another) while the cut parameter of the algorithm remains constant.

If the radial rapidity ρ_{ik} between two preclusters which is related to b_{ik} by

$$b_{ik} = -2 + 2 \operatorname{ch}(\rho_{ik}), \quad \text{where} \quad \rho_{ik} = \operatorname{arcch} \left(\frac{m_{ik}^2 - m_i^2 - m_k^2}{2m_i m_k} \right) \quad (3)$$

is used as metric, the obtained algorithm will be absolutely identical to the B algorithm as only the coefficients, which do not vary from iteration as well as the cut parameter of the algorithm, enter into expression (3).

Only charged pions were used in the analysis of the experimental data on $\pi^- + p$ and $\pi^- + C$ interactions at 40 GeV/c [7] in order to study spectator jets in the fragmentation region of beam and target particles. However, the jets formed by fragmenting quarks, diquarks and gluons contain all possible particles, although they are mainly charged pions and photons from the decays of neutral pions. Of course, the restriction on masses equality of particles involved in the analysis for a search and for reconstruction of jets is not essential to the binary B and JADE algorithms. When the B and JADE algorithms operate (even at mass equality of all particles involved in the analysis), the masses of preclusters vary and can only grow with increasing number of iterations. On the other hand, the restrictions on mass equality of particles involved in the analysis for the reconstruction of hadron jets can be essential using the A_n algorithm (see, for example, [9, 15]).

As for the binary B algorithm, the use of protons, in addition to pions, in the analysis for a search for jets improves the performances and properties of the reconstructed jets and also brings about the detection of jet leadership properties and their internal structure. In particular, well marked resonant structures associated with Δ isobars show themselves in the effective mass distributions of jets reconstructed by the B algorithm.

Figure 1 shows the dependence of N_J -events as the numbers of events 0, 1, 2, 3 and so on (further, it is denoted by symbol J) in $\pi^- + p$ and $\pi^- + C$ interactions at 40 GeV/c reconstructed on the basis of the B algorithm, on the cut parameter of the algorithm, b_{cut} . In the analysis, all events were taken into account in which the total number of pions and protons in the final state is equal to ≥ 2 . The dependence of the sizes of R and L jets, b_R and b_L , and also the distance between them b_{RL} in 4-velocity space on the cut parameter b_{cut} in two- and multi-jet $\pi^- + p$ and $\pi^- + C$ events are shown in Fig. 2. The dependence of the masses of R and L jets and the mass of a two- and multi-jet system m_{RL} on the cut parameter b_{cut} in two- and multi-jet $\pi^- + p$ and $\pi^- + C$ events are also presented in Fig. 2.

Let the jet J , where $J = R$ or L , consist of N_{\pm}^J particles with 4-momentum p_j^{\pm} , where $J = 1, 2, \dots, N_j$, here N_J is the number of the jet in each event. Then the quantities b_J , m_J , b_{RL} and m_{RL} are defined by the expressions

$$b_J = \frac{2}{N_{\pm}^J(N_{\pm}^J - 1)} \sum_{i=1}^{N_{\pm}^J} \sum_{k>i}^{N_{\pm}^J} b_{ik}, \quad m_J^2 = P_J^2, \quad P_J = \sum p_j^{\pm}; \quad (4)$$

$$b_{RL} = - \left(\frac{P_R}{m_R} - \frac{P_L}{m_L} \right)^2, \quad m_{RL}^2 = (P_R + P_L)^2. \quad (5)$$

A comparison of the distributions for $\pi^- + p$ and $\pi^- + C$ collisions with similar ones presented

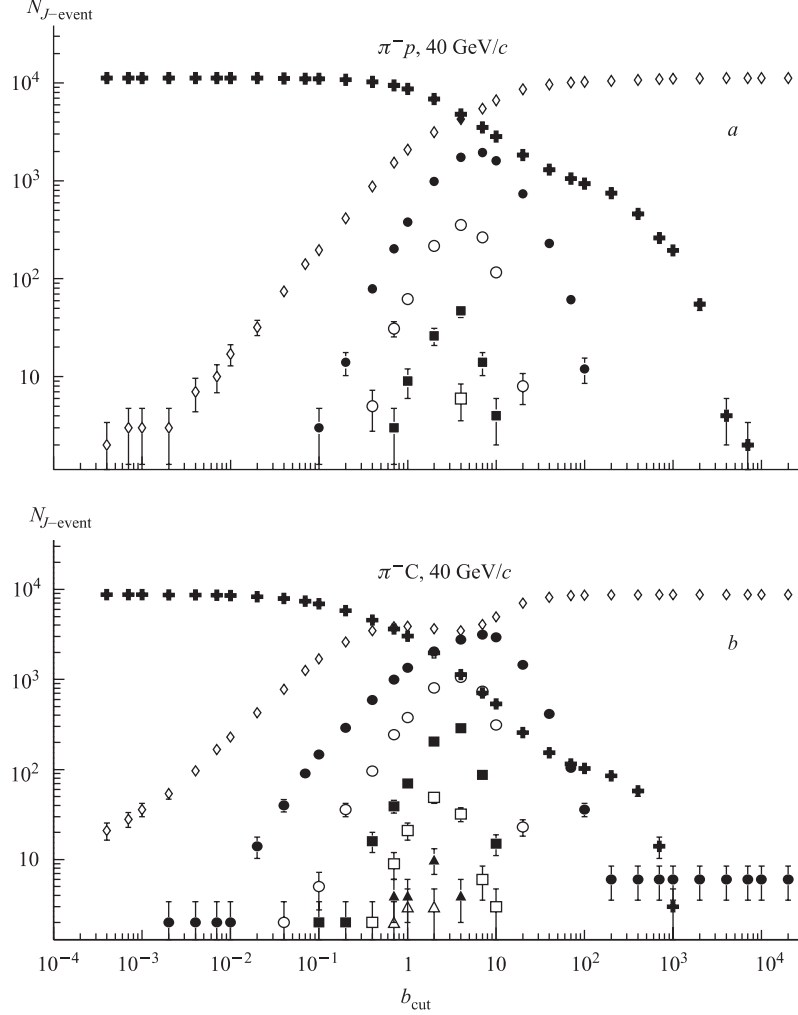


Fig. 1. Dependence of the number $N_{J\text{-event}}$ of mixed N -jet events on cut parameter b_{cut} for $\pi^- + p$ (a) and $\pi^- + C$ interactions (b): \oplus — 0 jet event; \diamond — 1 jet; \bullet — 2 jet; \circ — 3 jet; \blacksquare — 4 jet; \square — 5 jet; \blacktriangle — 6 jet; \triangle — 7 jet

in Figs. 1 and 2 [7] shows that the participation of protons in a jet practically does not affect the jet size and the character of jet dependence on the value of parameter b_{cut} .

Thus, we have $b_{\text{cut}} = 10\text{--}20$ hadron jets as well as for π^\pm meson jets as the relation $N_3/N_2 = 0.01$ and 0.07 at $b_{\text{cut}} = 20$ and 10 , respectively (see also [7]). Note that the number of two-jet events N_2 reaches a maximum at $b_{\text{cut}} = 5$ in $\pi^- + p$ interactions and at $b_{\text{cut}} = 10$ in $\pi^- + C$ interactions. Proceeding from this, in some cases we use the value of parameter b_{cut} in an interval $5 < b_{\text{cut}} < 20$ to increase the number of two-jet events.

Out of the total number 11501 (8791) events in $\pi^- + p$ ($\pi^- + C$) interactions we have only 11209 (8740) events in which the total number of pions and protons in the final state is ≥ 2 .

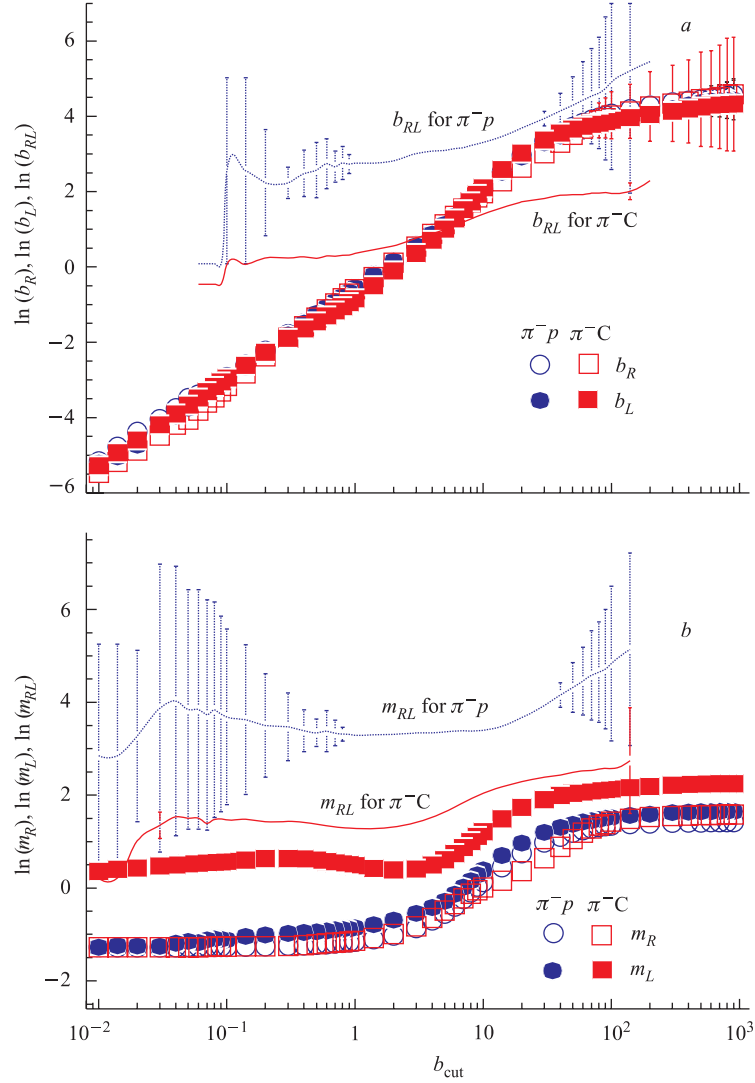


Fig. 2. Dependence of the characteristics of the right (R) and left (L) jets consisting of protons and pions in all jet events reconstructed by the B algorithm on cut parameter b_{cut} . a) b_R and b_L are the sizes of the R and L jets and b_{RL} is the distance between the R and L jets in 4-velocity space of two- and multi-jet system (the values of b_R , b_L and b_{RL} are calculated by a logarithm scale); b) m_R and m_L are the masses of the R and L jets and m_{RL} is the effective mass of two- and multi-jet system (the values of m_R , m_L and m_{RL} are calculated by a logarithm scale too)

Thus, for $b_{\text{cut}} = 10$ we have $N_0 = 2838(2462)$ zero-jet events, $N_1 = 6649(8502)$ one-jet events, $N_2 = 1602(2978)$ two-jet events, $N_3 = 116(270)$ three-jet events and $N_4 = 4(12)$ four-jet events. For the $b_{\text{cut}} = 20$ we have $N_0 = 1836(1424)$, $N_1 = 8630(11357)$, $N_2 = 736(1424)$ and $N_3 = 8(20)$, $\pi^- + p(\pi^- + C)$, respectively. Figure 3 shows dependence

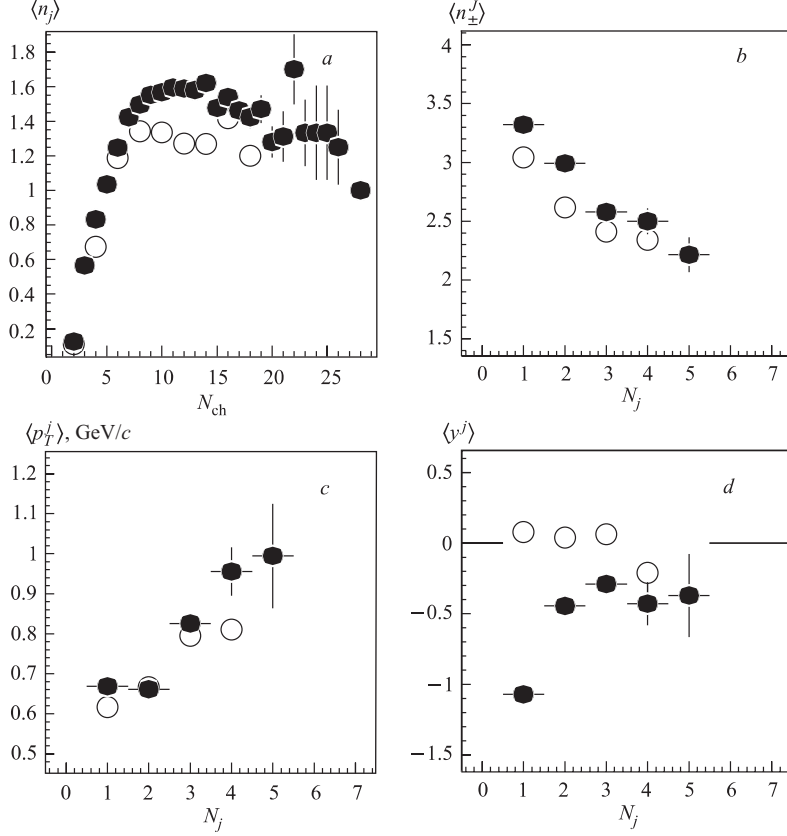


Fig. 3. Some average jet characteristics dependence. An average jet number $\langle n_j \rangle$ dependence on total charged multiplicity N_{ch} of each event (a), an average particle number in a jet $\langle n_{\pm}^J \rangle$ dependence (b), an average jet transverse momentum $\langle p_T^J \rangle$ dependence (c) and an average jet rapidity $\langle y^J \rangle$ dependence (d) on a jet number N_j

of some average jet characteristics in $\pi^- + p$ and $\pi^- + C$ interactions. The behavior of the dependence of the average jet numbers, $\langle n_j \rangle$, on total multiplicity N_{ch} increases to the values that are equal to the average particle numbers n_{ch} presented in Tables 1 and 2, i.e., $\bar{n}_{ch}^{\pi p} = 5.6 \pm 0.1$ and $\bar{n}_{ch}^{\pi C} = 8.7 \pm 0.1$. In $N_{ch} > \langle \bar{n}_{ch}^{\pi p} \rangle (\langle \bar{n}_{ch}^{\pi C} \rangle)$ regions the values of $\langle n_j \rangle$ are constant and equal to $\langle n_j \rangle \sim 1.3 \div 1.4$ for $\pi^- + p$ and to ~ 1.6 for $\pi^- + C$ interactions. As can be seen from Fig. 3 their mean characteristic values, i.e., $\langle n_{\pm}^J \rangle$, $\langle p_T^J \rangle$ and $\langle y^J \rangle$ for $J \geq 3$, possess the features different from one- and two-jet events. Figure 4 presents longitudinal momentum p_z^J distributions of R and L jets from one-, two- and multi-jet events in $\pi^- + p$ and $\pi^- + C$ interactions at $b_{cut} = 10$. The results show that two well-separated jets are observed.

Tables 1 and 2 present the average values of particle charge and multiplicity in a jet and also the correlation parameter of two jets in two- and multi-jet events at $b_{cut} = 10$. These data are presented without protons involved in the analysis for search for a jet and also with

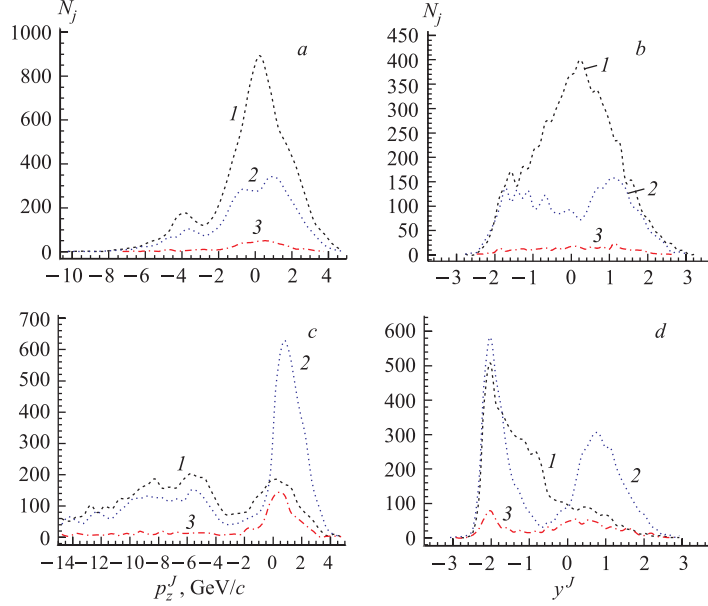


Fig. 4. Longitudinal momentum p_z^J (a, c) and rapidity y^J (b, d) distributions of R and L jets in c.m.s. from one- (1), two- (2) and multi-jet (3) events in $\pi^- + p$ (a, b) and $\pi^- + C$ (c, d) interactions at $b_{\text{cut}} = 10$. Both pions and protons are involved in the jets

Table 1. The average characteristics of a jet from one-, two- and multi-jet events in $\pi^- + p$ interactions at $b_{\text{cut}} = 10$. For L jets the quantity θ_L is calculated via $180^\circ - \theta_L$. 11501 $\pi^- + p$ events ($\bar{n}_{\text{ch}} = 5.6$), 10218 jets with $N(\pi^-, \pi^+, p) \geq 2$ ($\langle n_j \rangle = 0.91 \pm 0.01$)

The value (dimension)	One-jet event ($N_j = 1$)		Two-jet event ($N_j = 2$)		Multi-jet event ($N_j \geq 3$)	
	L_1 jet	R_1 jet	L_2 jet	R_2 jet	$L_{\geq 3}$ jet	$R_{\geq 3}$ jet
n_{\pm}^J	4.3	4.3	3.0	2.9	2.6	2.4
Q_j	0.34	-0.25	0.35	-0.31	0.19	-0.28
b_j	9.2	9.1	6.0	5.8	4.7	4.5
T_k , GeV	0.123	0.110	0.078	0.068	0.057	0.048
m_j , GeV/c^2	1.74	1.37	1.03	0.72	0.77	0.51
p_T^j , GeV/c	0.617	0.618	0.643	0.690	0.784	0.806
x_F^j	-0.42	0.31	-0.48	0.34	-0.42	0.27
θ^j , deg	32	33	29	32	38	41
Δ , deg	—		1.5	1362 events with R and L jets	2.6	239 events with R and L jets
b_{RL}	—		26		33	
m_{RL} , GeV/c^2	—		4.1		3.5	
N_j	3038	3611	1541	1662	170	195

Table 2. The average characteristics of a jet from one-, two- and multi-jet events in $\pi^- + C$ interactions at $b_{\text{cut}} = 10$. For L jets the quantity θ_L is calculated via $180^\circ - \theta_L$. 8791 $\pi^- + C$ events ($\bar{n}_{\text{ch}} = 8.7$), 11822 jets with $N(\pi^-, \pi^+, p) \geq 2$ ($\langle n_j \rangle = 1.35 \pm 0.01$)

The value (dimension)	One-jet event ($N_j = 1$)		Two-jet event ($N_j = 2$)		Multi-jet event ($N_j \geq 3$)	
	L_1 jet	R_1 jet	L_2 jet	R_2 jet	$L_{\geq 3}$ jet	$R_{\geq 3}$ jet
n_{\pm}^j	6.6	4.7	4.6	3.4	3.7	2.5
Q_j	1.92	-0.08	1.80	-0.21	1.40	-0.30
b_j	10.1	9.1	6.0	6.9	4.9	4.6
T_k , GeV	0.159	0.101	0.106	0.077	0.076	0.047
m_j , GeV/c ²	4.00	1.50	2.78	0.95	1.86	0.55
p_T^j , GeV/c	0.675	0.671	0.657	0.683	0.953	0.832
x_F^j	-1.88	0.30	-1.97	0.31	-1.55	0.24
θ^j , deg	10	35	11	33	27	45
Δ , deg	—		25 } 2691 events	23 } 653 events		
b_{RL}	—		27 } with	39 } with		
m_{RL} , GeV/c ²	—		8.0 } R and L jets	6.5 } R and L jets		
N_j	4150	790	3124	2750	525	483

protons in the final state. As a correlation parameter of jets in two- and multi-jet events, the quantity $\Delta = 180^\circ - \theta_R - \theta_L$ is taken where θ_R and θ_L are the polar angles of R and L jets relative to the direction of the momentum of an initial pion in the center-of-mass system of $\pi^- + p$ interactions. The results presented in Tables 1 and 2 will be discussed in detail in the following section of this article. However, it should be noted that the proton component of a jet involved in the analysis for a search for jets in conjunction with the pion component improve the correlation of two jets and also approaches the value of jet charge to those expected in the framework of quark representations. Thus, the multiplicity of particles in jets practically does not vary.

2. UNIVERSALITY OF HADRON JETS IN JET EVENTS

This section is devoted to the analysis of the characteristics of mixed spectator jets in one-, two- and multi-jet events reconstructed on the basis of the B algorithm. The results of the analysis of the experimental data on $\pi^- + p$ and $\pi^- + C$ interactions obtained with the 2-m propane bubble chamber of JINR exposed to a beam of negative pions with a momentum of 40 GeV/c at the IHEP (Serpukhov) accelerator are presented. As distinct from [7], not only pions but also protons in a final state were used to reconstruct jets in the beam and targets fragmentation regions. As was already mentioned, the proton component of a jet involved in the analysis in addition to the pion one does not change significantly the value of the B algorithm cut parameter b_{cut} whose values are within limits $10 < b_{\text{cut}} < 20$. At $b_{\text{cut}} > 20$ in two-jet events there are well separated jets, while jet separation at $b_{\text{cut}} \cong 10$ is not so precise as at $b_{\text{cut}} \sim 20$, but the number of two-jet events is much larger. At the values of b_{cut} in an

interval of $10 < b_{\text{cut}} < 20$, all events with jets are divided into two groups: one- and two-jet events. The number of three-jet events is much smaller.

In one-jet events, the jet with $\cos \theta_j > 0$, where θ_j is the jet angle relative to the collision axis in the $\pi^- + p$ center-of-mass system (this is a jet in the beam fragmentation region), will be called an R_1 jet and the jet with $\cos \theta_j < 0$, i.e., a jet in target fragmentation region, an L_1 jet. In two- and multi-jet events, R_2 and L_2 jets are determined from the condition $y_R > 0$ and $y_L < 0$; i.e., the jet with a large rapidity value is an R_2 jet and another one is an L_2 jet.

Tables 1 and 2 present the characteristics of R and L jets in one-, two- and multi-jet events and also the numbers N_J of one-jet ($J = 1$), two-jet ($J = 2$) and multi-jet ($J \geq 3$) events at $b_{\text{cut}} = 10$ in $\pi^- + p$ and $\pi^- + C$ interactions. Thus, $J = R$ or L also designates a right or left jet, respectively. Here, the N_{\pm}^J is the multiplicity of particles in a jet, Q_j and m_j are the jet charge and mass, respectively, p_T^J and x_F^J are the jet transverse momentum and a part of its longitudinal momentum in the $\pi^- + p$ center-of-mass system, respectively. The size of a jet in 4-velocity space is defined by quantity b_j (see expression (4)) which can be interpreted as a jet diameter. Such a definition of the jet size is convenient because it does not require defining the jet center in velocity space. In [8] the jet size in velocity space is defined by quantity b_k related to quantities b_j and N_j by the expression (see [7])

$$b_k = -2 + 2\sqrt{\left(1 + \left(1 - \frac{1}{N_j}\right)\frac{b_j}{2}\right)} \quad \text{or} \quad b_k = -(V - u_k)^2. \quad (6)$$

The quantity b_k can be interpreted as a jet radius in velocity space as b_k is the distance between the particle and the jet center averaged over all particles involved in the jet.

The quantity T_k is the kinetic energy of the particle in the jet rest frame. It is easy to define a formula $T_k = mb_k/2$. Tables 1 and 2 give the average values of quantities b_j and T_k .

In one-jet events, the multiplicity of particles in the R and L jets equals $N_{j1} = 4.3$ at $b_{\text{cut}} = 10$, and it is one unity larger than the corresponding value in two-jet events ($N_{j2} \cong 3.0$). Moreover, such characteristics as jet mass m_j and its size b_j (or T_k) in one-jet events are much larger than those in two- and multi-jet ones. This circumstance apparently specifies that one-jet events are those in which the second spectator jet or at least its central or leading part does not consist of more than one charge particle (pion or proton).

Thus, charged pions and protons, which can be around the periphery or on the tail of such an «invisible» jet, can get to the reconstructed jet consisting of pions and protons and increase the average multiplicity of particles in the R and L jets of one-jet events. It is natural that such peripheral or «strange» pions and protons will increase both the mass and size of jet in velocity space as they are from an opposite jet. Nevertheless, unlike the multiplicity of particles in a jet, its mass and size, such main kinematics characteristics of R and L jets as transverse momentum p_T^J , a part of longitudinal momentum x_F^J and emission angle θ^J in one-, two- and multi-jet events are rather close and differ by no more than 10–15% at $b_{\text{cut}} = 10$. Here the results of x_F^J , θ^J for left one- and two-jet events do not relate. Nearness of such jet characteristics from one-, two- and multi-jet events can be also used as a criterion to select the algorithm cut parameter $b_{\text{cut}} = 10$. As b_{cut} increases, the characteristics of jets from two- and multi-jet events approach, as much as possible, the values expected in the framework of quark-parton model. Thus, the discrepancy between the characteristics of jets

from one- and two-jet events increases. This is a consequence of that all events are interpreted as one-jet ones at $b_{\text{cut}} \rightarrow \infty$.

Now let us turn to the comparison of the characteristics of R and L jets among themselves from one- and two-jet events, i.e., R_1 with L_1 and R_2 with L_2 . It is possible to find out that the values of particle multiplicity in a jet, jet size and transverse momentum are identical, but the values of jet charge, mass and longitudinal variable x_F are significantly different for R and L jets. The distributions of the last quantities bear a mark of the quark structure of particle fragmenting into an R and L jets, i.e., a beam or target particle. We have $Q_{R1} = -0.25$, $Q_{R2} = -0.31$ and $Q_{R3} = -0.28$ at $b_{\text{cut}} = 10$ for an R jet (fragmenting region of a beam pion), while we have $Q_{L1} = 0.34$, $Q_{L2} = 0.35$ and $Q_{L3} = 0.19$ for an L jet (fragmenting region of a target proton). Taking into account the quark composition of pion and proton, one can determine the average quark charge in the pion and proton fragmentation region: $Q_R = (Q_{\bar{u}} + Q_d)/2 = -0.5$ and $Q_L = (2Q_u + Q_d)/3 = 1/3$, where Q_q is the quark/antiquark charge.

In the longitudinal momentum distributions of L jets (proton fragmentation region), maximum is observed in the region of jet longitudinal momentum $p_z^J \approx -4$ GeV or rapidity $y^J \approx -2$ which is connected with proton diquark exists in fragmentation into an L jet (see Fig. 3). Such a characteristic of diquark structure exists in the inclusive spectra of leading baryons formed on proton diquark [16, 17]. The presence of a diquark maximum gives an increase of x_F^J for L jets in view of the proton component of a jet.

The jet mass is a third variable which differs significantly for R and L jets in $\pi^- + p$ and $\pi^- + C$ interactions. Figure 4 presents a particular structure in the mass distributions of R and L jets one-, two- and multi-jet events reconstructed by the B algorithm. The next section of this paper is devoted to detailed analysis of the mass spectra of jets from one-, two- and

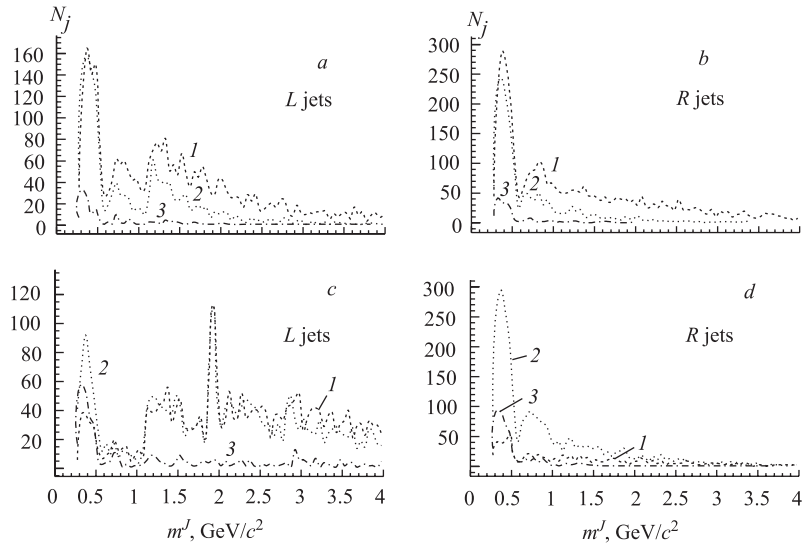


Fig. 5. Mass distributions of the R and L jets from one- (1), two- (2) and multi-jet (3) events in $\pi^- + p$ interactions (a, b) and $\pi^- + C$ interactions (c, d). The jets are reconstructed by the B algorithm at $b_{\text{cut}} = 10$ and consist of pions and protons

multi-jet events. Here it should be only stressed that this structure is different for R and L jets and associated with the type of a particle fragmenting into a jet. Note that there is no other structure similar to those presented in the mass distributions of R and L jets (see Fig. 5) if the JADE algorithm is used for jet reconstruction (see Fig. 6 from [18]).

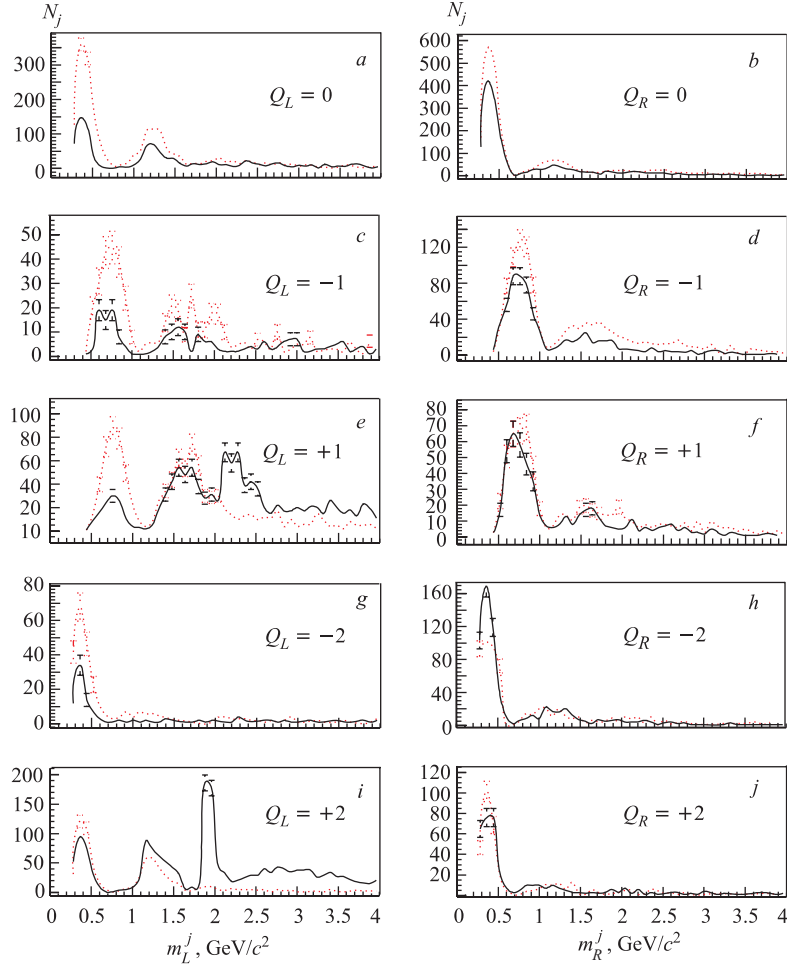


Fig. 6. The total mass distributions of mixed L (a , c , e , g , i) and R (b , d , f , h , j) jets with various values of an electric charge from jet events in $\pi^- + p$ ($\pi^- + C$) interactions. The jets are reconstructed by the B algorithm at $b_{\text{cut}} = 10$ and consist of pions and protons. The values of jet charges are given in the corresponding figures

From the foregoing it follows that the properties of R and L jets are universal with a precision of 10–15% in one- and two-jet events. A noticeable difference in particle multiplicity in jets, their sizes and masses is due to «other» particles involved in jet from one-jet events. It is also shown that the values of jet charge, mass and a part of longitudinal momentum greatly depend on the quark composition of particle fragmenting onto a jet. However, particle

multiplicity in a jet, size and transverse momentum do not depend on the fragmentation region and they are identical for R and L jets. Let us also note that the specified circumstances are valid only for R and L jets reconstructed by the B algorithm, while the characteristics of jets reconstructed by the JADE algorithm do not reflect the quark composition of particle fragmenting into a jet. In this case the multiplicity of particles in the jets is much larger than that for jets reconstructed by the B algorithm. This specifies that the jets reconstructed by the JADE algorithm are strongly overlapped (see also [7]).

3. SEPARATION OF HADRON JETS BY VALUES OF AN ELECTRICAL CHARGE

As was already noted, the particular structure takes place in the mass distributions of R and L jets, which is different in the fragmentation region of pion (R jet) and proton (L jet). This structure becomes more particular if jets are separated by the value of electrical charge Q_R and Q_L . Figure 5 presents the mass distributions of R and L jets with values of electrical charge from one- and two-jet $\pi^- + p$ and $\pi^- + C$ events reconstructed by the B algorithm at $b_{\text{cut}} = 10$.

Figure 6 shows that the proton component involved in the analysis has no practical influence on the mass distributions of R jets at charge values $Q_R = 0, \pm 1, \pm 2$ and also on the mass distributions of L jets at $Q_L = -2$. However, significant differences with/without taking into account protons in a jet are observed in the mass distributions of L jets at $Q_L = 0, \pm 1$ and ± 2 . These differences are connected with the mass region of Δ resonances at $Q_L = 0 (\Delta^0 \rightarrow p\pi^-)$ and $Q_L = 2 (\Delta^{++} \rightarrow p\pi^+)$ and the mass region of $\Delta^*(1600)$ resonances at $Q_L = \pm (\Delta^{*+} \rightarrow p\pi^-\pi^+$ and $\Delta^{*-} \rightarrow p\pi^-\pi^-)$.

The total mass distribution of L jets with charges $Q_L = 0$ and $+2$ is presented in Fig. 7, where there are only two particles in jets: one of them is a proton, and the other is a pion. All L jets satisfying the above requirements from one-jet and two-jet events in pp interactions reconstructed at $b_{\text{cut}} = 6$ are taken into account in this distribution. Here the results of fitting the distributions by the Breit–Wigner formula are also presented:

$$W(M) = \frac{\text{const}}{(M - M_{\text{res}})^2 + (\Gamma_{\text{res}}/2)^2}. \quad (7)$$

Here $M_{\text{res}}, \Gamma_{\text{res}}$ and const are respectively the mass, width and normalization factor which are connected with the fit parameters $M_{\text{res}}, \Gamma_{\text{res}}$ and const presented in the same figure. Note that the values of M_{res} and Γ_{res} vary respectively from 1.22 to 1.25 GeV and from 0.21 to 0.40 GeV with changing the parameter b_{cut} over an interval of $5 < b_{\text{cut}} < 15$.

Figure 8 presents the mass distributions of L jets for $Q_L = \pm 1$ on condition that there are three particles in a jet: one of them is proton and the two other are pions. This mass distribution of L jets from one- and two-jet events in $\pi^- p$ interactions is reconstructed at $b_{\text{cut}} = 8$. The results of fitting by the Breit–Wigner formula are also presented in Fig. 7. Changing the parameter b_{cut} over an interval of $5 < b_{\text{cut}} < 15$, the values of M_{res} and Γ_{res} vary from 1.50 to 1.78–0.52 GeV, respectively. The results of fitting apparently specify that the resonance $\Delta^*(1600)$ is observed in jets at $Q_L = \pm 1$ as its channel $N_{\pi\pi}$ branching is equal to 75–90%, while the channel N_{π} branching 10–25%. This circumstance can be the reason that this resonance is not observed at $Q_L = 0$ and $+2$. As for N^* resonances, it is

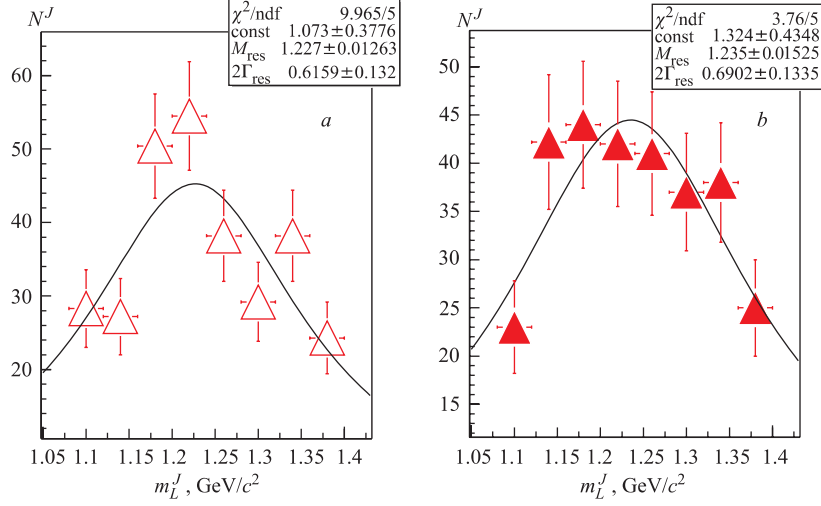


Fig. 7. The total mass distribution of left (L) jets with charges $Q = 0$ and $+2$ consisting of one proton and one charged pion from one- and two-jet events in $\pi^- p$ (a) and $\pi^- C$ (b) interactions. The jets are reconstructed by the B algorithm at $b_{\text{cut}} = 6$. The fit results by the resonant Breit-Wigner formula are also presented. The bin width in the histogram is equal to 40 MeV

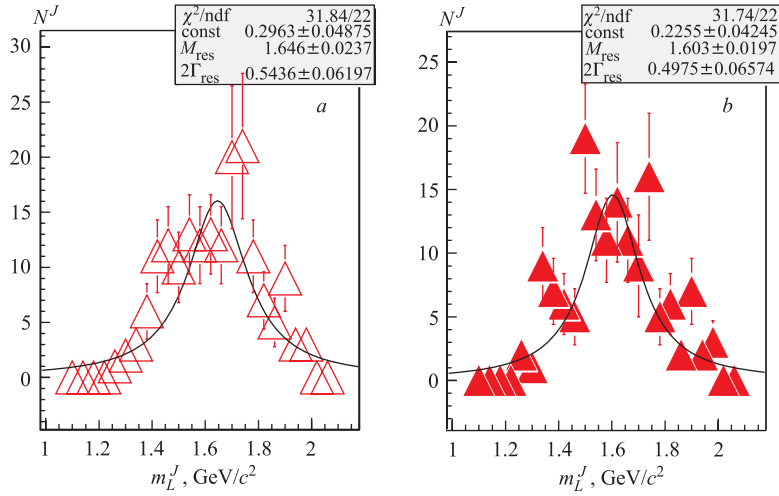


Fig. 8. The total mass distribution of left (L) jets with charges $Q = -1$ and $+1$ consisting of one proton and two charged pions from one-jet events in $\pi^- p$ (a) and $\pi^- C$ (b) interactions. The jets are reconstructed by the B algorithm at $b_{\text{cut}} = 8$. The fit results by the resonant Breit-Wigner formula are also presented. The bin width in the histogram is equal to 40 MeV

possible to note that their contribution to the channel $N_{\pi\pi}$ branching is far smaller than for the $\Delta^*(1600)$ resonance.

Besides the features in the mass distributions of jets associated with Δ isobars or $\Delta^*(1600)$ resonances, Fig. 6 presents some additional features at $Q_j = 0$ and ± 2 in the mass region of jet $2m_\pi < m_J < 0.6$ GeV and also in the mass region of jet $3m_\pi < m_J < 1.1$ GeV and $(m_p + 2m_\pi) < m_J < 2.2$ GeV at $Q_j = \pm 1$. For $\pi^- + C$ interactions on mass R and L jets at $b_{\text{cut}} = 10$ are presented in Fig. 6. In the case additionally to a feature for $\pi^- + p$ interactions at $Q_L = 2$ there are features in the mass region of jets $2m_p < m_J < 2.2$ GeV and also at $Q_L = 1$ in the mass region of jets $(2m_p + m_\pi) < m_J < 2.8$ GeV.

At first, we shall consider the features at $Q_j = 0$ and ± 2 in the mass region of a jet $2m_\pi < m_J < 0.66$ GeV. From expression (2) it follows that the mass of jets consisting of pions and reconstructed by B algorithm at $b_{\text{cut}} = 10$ satisfies a requirement $2m_\pi < m_J < m_\pi \sqrt{4 + b_{\text{cut}}} = 0.52$ GeV. Thus, the jets consisting of two pions and reconstructed at $b_{\text{cut}} = 10$ fill in a mass region with the interval from $2m_\pi$ to $m_\pi \sqrt{4 + b_{\text{cut}}}$. It is necessary to note that the upper limit in the distribution on mass of all possible two-pion combinations is wider than the quantity $m_\pi \sqrt{4 + b_{\text{cut}}} - 2$.

Now let us consider the features at $Q_j = \pm 1$. In this case, the masses of jets consisting of three pions and reconstructed by the B algorithm at $b_{\text{cut}} = 10$ satisfy the requirement

$$3m_\pi < m_J m_\pi \sqrt{5 + b_{\text{cut}} + (2 + b_{\text{cut}}) \sqrt{4 - b_{\text{cut}}}}. \quad (8)$$

Deriving (8) for the upper limit of m_J , we mean that the limitation on effective masses $m_{12} < m_\pi \sqrt{4 + b_{\text{cut}}}$ takes place at least for one pair of π from a three-pion jet. This is a direct consequence of logic construction of the B algorithm. At $b_{\text{cut}} = 10$ we find $3m_\pi < m_J < 1.08$ GeV from expression (8). This is in agreement with the distributions presented in Fig. 7.

So far we have considered the features in the mass distributions of two- and three-particle jets consisting of particles with an identical mass (namely, of pions or protons). For two-particle jets, there are such jets as (πp) and for three-particle jets they are $(\pi\pi p)$ and $(\pi p p)$.

For the case of two-particle mixed jets with $Q_L = 0$ and ± 2 reconstructed at $b_{\text{cut}} = 10$, we have $(m_\pi + m_p) < m_j < \sqrt{(m_\pi + m_p)^2 + m_\pi m_p b_{\text{cut}}} = 1.58$ GeV. For the mass m_J of three-particle mixed jets reconstructed by the B algorithm at $b_{\text{cut}} = 10$, the following limitation can be obtained:

$$m_1 + m_2 + m_3 < m_j < \sqrt{(m_3 + m_{12(\text{max})})^2 + m_3 m_{12(\text{max})} b_{\text{cut}}}, \quad (9)$$

where $m_{12} = \sqrt{(m_1 + m_2)^2 + m_1 m_2 b_{\text{cut}}}$. In consequence of that at first particles 1 and 2 are united in precluster 12 and particle 3 joins precluster 12.

For the masses of such three-particle mixed jets as $(\pi\pi p)$ at $b_{\text{cut}} = 10$, we have $(2m_\pi + m_p) < m_{\pi\pi p} < 2.7$ GeV. In this case, there are two pictures of $(\pi\pi p)$ formation: (i) at first the precluster $(\pi\pi)$ is formed and the proton is associated with it and (ii) at first the precluster (πp) is produced and then the second pion is associated with it. For the first case, we have $m_{(\pi\pi)p} < 2.7$ GeV from expression (9) and for the second case $m_{(\pi p)\pi} < 2.3$ GeV. For the masses of three-particle mixed jets such as $(\pi p p)$ at $b_{\text{cut}} = 10$, we find $(m_\pi + 2m_p) < m_{\pi p p} < 4.6$ GeV. In this case $m_{(\pi p)p} < 4.6$ GeV and $m_{(pp)\pi} < 4.3$ GeV. Figures 7 and 8 present all these features in the mass distributions of L jets at $Q_L = 0, \pm 1$ and 2.

Thus, one can draw the following conclusion: all the structures in the mass distributions of jets in Figs. 7 and 8 (except the structures in the regions of Δ isobars and $\Delta^*(1600)$)

resonances) are not physical and their occurrence is caused by the B algorithm used for jet reconstruction. As for the features at $Q_L = 0$ and 2 in the mass region of $\Delta(1232)$ resonance and at $Q_L = \pm 1$ in the region of $\Delta^*(1600)$ resonance, one can assume contributions from these resonances relative to background. Thus, the intensification of the resonance contribution will take place in the case where the average distance between the resonance and the particle nearest to it in velocity space is larger than that for the case of a background system relative to the resonance.

In this case we only want to show that the hadron jets reconstructed by the B algorithm have an appreciable internal (probably resonant) structure and this structure is defined by the particle fragmenting into these jets. The jets reconstructed in this way carry information on their «parents»; that is, they have a leadership property in the fragmentation region of interacting particles.

Thus, the B algorithm reconstructs jets or a leading central part of the jet inside which particles are genetically bound by the mechanism of their formation. Note once again that the jets reconstructed by the JADE algorithm do not have this property.

4. AZIMUTHAL ANISOTROPY AND CORRELATIONS

The azimuthal anisotropy of final-state hadrons in noncentral nuclear collisions [19] is sensitive to the system evolution at early times [20]. At high p_T a hydrodynamical description of the hadron production mechanism may break down as process involving hard scattering of the initial-state partons as expected to play the dominant role. Large transverse momentum partons in the high-density system result from the initial hard scattering of nucleon constituents. After a hard scattering, the parton fragments create a high energy cluster (jet) of particles.

Hard scattering processes have been established at the high transverse momentum in elementary collisions at high energy through the measurement of jets [21–23], correlated back-to-back jets (dijets) [24], high- p_T single particles, and back-to-back correlations between high- p_T hadrons [25]. Jets have been shown to carry the momentum of the parent parton [26].

Correlations localized in both rapidity and azimuthal angle are characteristic of high-energy partons fragmenting into jets of hadrons. Such short-range correlations may be isolated from elliptic flow using two-particle correlation analysis performed in different regions of relative rapidity. Elliptic flow at RHIC can be described by a hydrodynamical model for p_T up to 2 GeV/ c [27].

Recently the STAR collaboration has measured the strength of back-to-back high- p_T charged hadron correlations, and observed a small suppression of the back-to-back correlation strength in peripheral collisions and nearly complete disappearance of back-to-back correlation in central Au + Au events [28].

Figure 9 shows the two-particle azimuthal normalized distributions with three different rapidity regions for $\pi^- + p$ and $\pi^- + C$ collisions, respectively: the first region is the window of rapidity absolute values $|\Delta y| < 0.5$, the second $0.5 < |\Delta y| < 1.5$, and the third $|\Delta y| > 1.5$. In the both $\pi^- + p$ and $\pi^- + C$ interactions there are the azimuthal correlations due to momentum conservation, dijets and resonance, decays and the back-to-back correlations, and these correlations were experimentally investigated [29].

There is an enhancement near $\Delta\phi = 0$ in the small relative rapidity correlation behavior that may be evidence of hard scattering for the first region of $\pi^- + p$ interactions and fragmen-

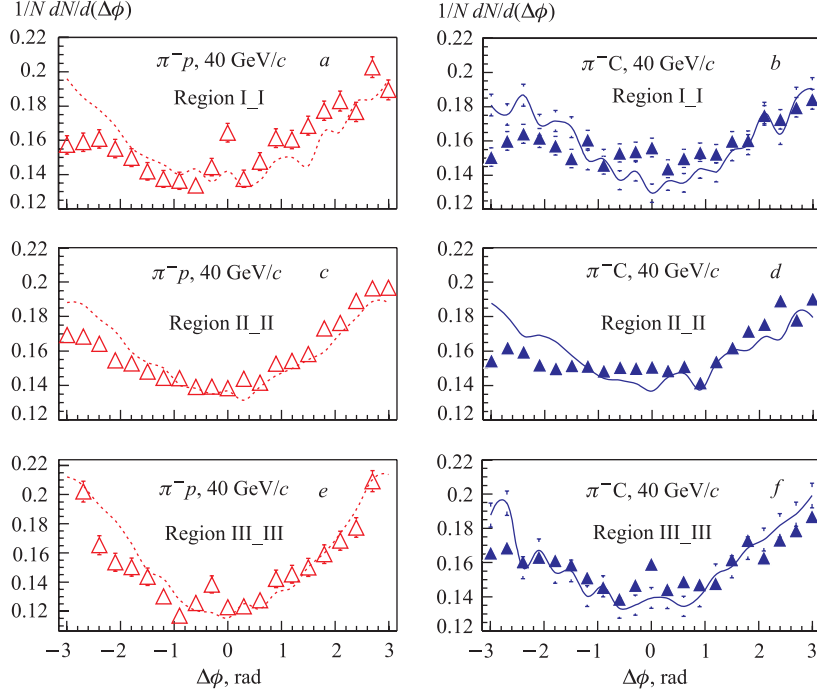


Fig. 9. Charged hadron azimuthal distributions for $\pi^- + p$ and $\pi^- + C$ interactions. The open triangles are for $\pi^- + p$ and solid triangles for $\pi^- + C$ collisions. *a, b*) Correlation function for $|\Delta y| < 0.5$; *c, d*) for $0.5 < |\Delta y| < 1.5$; *e, f*) for $|\Delta y| > 1.5$. Dashed and solid curves are the calculations by FRITIOF simulation for $\pi^- + p$ and $\pi^- + C$ interactions, respectively

tation for the third region of $\pi^- + C$ collisions and this data was quantitatively agreed [29]. This enhancement is not in data of FRITIOF simulation. The FRITIOF and both $\pi^- + p$ and $\pi^- + C$ experimental data for third regions there are strongly back-to-back correlations. But these back-to-back correlations are found weakly in the experimental data of two particle azimuthal correlation from jet production (see Fig. 10, where the two-jet particle azimuthal normalized distributions in three different rapidity regions for $\pi^- + p$ and $\pi^- + C$ interactions are presented). Figures 9 and 10 show that the difference between the jet and inelastic azimuthal correlation behaviors is not the diversity between $\pi^- + p$ and $\pi^- + C$ collisions in the first rapidity region and is strong in the third rapidity region (see last column in Fig. 11).

CONCLUSION

1. It is shown that the participation of proton component, along with pion one, in jets improves the distributions of the spectator jets; i.e., it brings them closer to the values expected in the framework of the quark-parton presentations of the hadron structure. In this case, the value of cut parameter b_{cut} for the *B* algorithm is practically invariable, and it remains within $10 < b_{\text{cut}} < 20$.

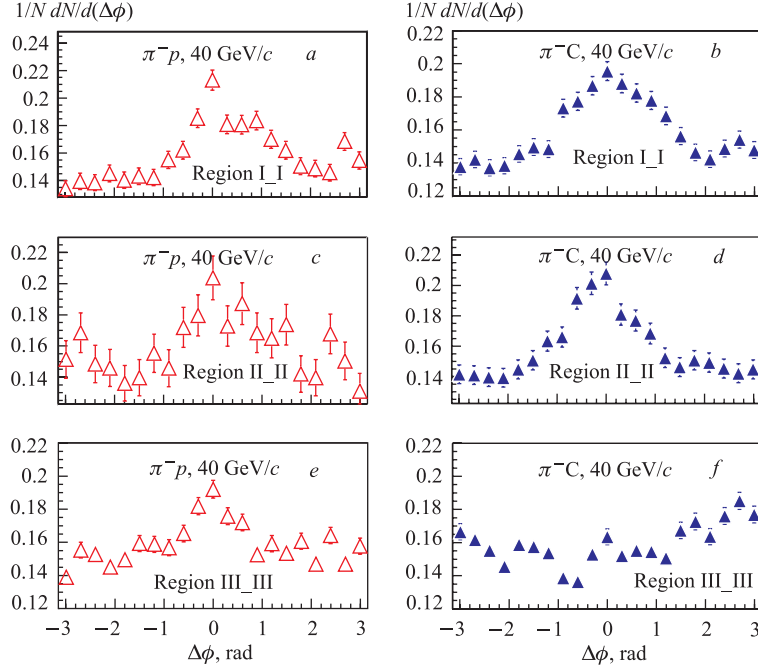


Fig. 10. Jet charged hadron azimuthal distribution for $\pi^- + p$ and $\pi^- + C$ interactions. The open triangles are for $\pi^- + p$ and solid triangles for $\pi^- + C$ collisions. *a, b*) Correlation function for $|\Delta y| < 0.5$; *c, d*) for $0.5 < |\Delta y| < 1.5$; *e, f*) for $|\Delta y| > 1.5$

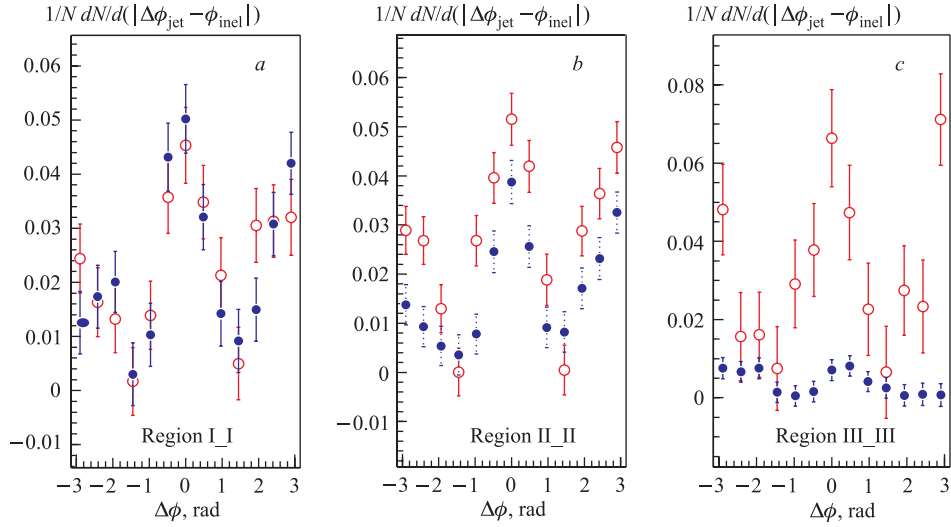


Fig. 11. Difference between the jet and inelastic azimuthal correlation in $\pi^- + p$ (O) and $\pi^- + C$ (●) collisions in three rapidity regions

2. It is found that the characteristics of $R(L)$ jets in one- and two-jet events differ from one another by less than 10–15% at $b_{\text{cut}} = 10$. This means that one-jet events are those where the second «invisible» jet consists of neutral particles and no more than one charged particle (pion or proton).

3. It is revealed that the sizes of jets in the fragmentation region of colliding π^- mesons and proton, their transverse momenta and particle multiplicity are similar, while jet charges, longitudinal momentum part and mass distributions depend on the quark composition of hadrons fragmenting into a jet.

4. The structures related to a hadron fragmenting into a jet are found in the mass distributions of L jets. At charge $Q_L = 0$ and ± 2 there are peaks connected with $\Delta^0(p\pi^-)$ and $\Delta^{++}(p\pi^+)$ resonances, respectively, and at $Q_L = \pm 1$ there are peaks connected with $\Delta^*(1600)$ resonances: $\Delta^{*+}(1600) \rightarrow (p\pi^+\pi^-)$ at $Q_L = +1$ and the states $\Delta^*(1600) \rightarrow (p\pi^-\pi^-)$ at $Q_L = -1$.

5. It is shown that the small azimuthal angle correlations provide direct evidence of hard scattering observed for the jets reconstructed by the B algorithm and fragmentation processes and a strong back-to-back correlation exists for $\pi^- + p$ and $\pi^- + C$ collisions.

Acknowledgements. The authors are grateful to the members of the whole 2-meter bubble chamber collaboration for the experimental materials. D.Sc. R. Togoo acknowledges the support from the German Academic Exchange Service (DAAD) and would like to thank his colleague Prof. J. Stachel for his invitation and hospitality in Heidelberg.

REFERENCES

1. Collins P. D. B., Martin A. D. // Rep. Prog. Phys. 1982. V. 45, No. 4. P. 335.
2. Fialkowski R., Kittel W. // Rep. Prog. Phys. 1983. V. 46, No. 11. P. 12283.
3. Badalian R. G., Gulkanian G. R. // Yad. Fiz. 1985. V. 41. P. 1611.
4. Ochs W. // Nucl. Phys. B. 1977. V. 118. P. 397.
5. Badalian N. N., Badalian R. G. // Z. Phys. C. 1990. V. 48. P. 587.
6. Badalian R. G., Korchagin S. A. // Yad. Fiz. 1990. V. 51. P. 1361.
7. Badalian N. N. et al. // JINR Rapid Commun. 1996. No. 1[75]. P. 27.
8. Baldin A. M. et al. // Nucl. Phys. A. 1985. V. 434. P. 695.
9. Baldin A. M. et al. // Yad. Fiz. 1988. V. 48. P. 995.
10. Vodopyanov A. S., Sadovski A. B. // JINR Rapid Comm. 1994. No. 5[68]. P. 21.
11. Angelov N., Lyubimov B. V., Togoo R. // Yad. Fiz. 1991. V. 45. P. 1316.
12. Bartel W. et al. // Z. Phys. C. 1986. V. 33. P. 23.
13. Bethke S. et al. // Phys. Lett. B. 1988. V. 213. P. 235.
14. Sjostrand T. LU TP 95-20. 1995; CERH-TH. 7112/93. 1993.

15. *Baldin A. M. et al.* // *Yad. Fiz.* 1989. V. 49. P. 1034; *Yad. Fiz.* 1990. V. 52. P. 1427;
Didenko L. A., Grishin V. G., Kuznetsov A. A. // *Proc. of the XVIII Intern. Symp. on Multiparticle Dynamics, Tashkent, 1987.* V. 45. P. 798.
16. *Badalian R. G., Gulkanian G. R., Korchagin S. A.* // *Yad. Fiz.* 1987. V. 45. P. 798.
17. *Badalian R. G.* // *Yad. Fiz.* 1989. V. 50. P. 1120.
18. *Badalian N. N., Badalian R. G., Kuznetsov A. A.* JINR Preprint P1-97-288. Dubna, 1997.
19. *Ollitrault J. J.* // *Phys. Rev. D.* 1992. V. 46. P. 229.
20. *Sorge H.* // *Phys. Rev. Lett.* 1997. V. 78. P. 2309.
21. *Banner M. et al.* // *Phys. Lett. B.* 1982. V. 118. P. 203.
22. *Arnison G. et al.* // *Phys. Lett. B.* 1983. V. 123. P. 115.
23. *Abe F. et al.* // *Phys. Rev. Lett.* 1989. V. 62. P. 613.
24. *Abe F. et al.* // *Phys. Rev. D.* 1990. V. 41. P. 1722.
25. *Arnison G. et al.* // *Phys. Rev. Lett. B.* 1982. V. 118. P. 173.
26. *Abe F. et al.* // *Phys. Rev. Lett.* 1990. V. 65. P. 968.
27. *Adler C. et al.* // *Phys. Rev. Lett.* 2003. V. 90. P. 032301.
28. *Adler C. et al.* // *Ibid.* P. 082302.
29. *Angelov N. et al.* // *Yad. Fiz.* 1977. V. 26, No. 1. P. 131; No. 5. P. 1029; *Yad. Fiz.* 1975. V. 22, No. 1. P. 122.

Received on September 14, 2004.